Connectivity and critical currents in polycrystalline MgB$_2$

M Eisterer, J Emhofer, S Sorta, M Zehetmayer and H W Weber

Atominstitut der Österreichischen Universitäten, Vienna University of Technology,
A-1020 Vienna, Austria

Abstract
Current transport in polycrystalline magnesium diboride is highly non-uniform (percolative) due to the presence of secondary phases and also due to the intrinsic anisotropy of the material. The influence of secondary phases on the transport properties of MgB$_2$ was investigated. Bulk samples were prepared from a mixture of MgB$_2$ and MgO powders by the *ex situ* technique in order to vary the MgO content systematically. The samples were characterized by resistive and magnetization measurements. The reduced MgB$_2$ fraction is modeled by a reduced effective cross section (connectivity), which was assessed directly by the experiments. The presence of MgO also increases the percolation threshold, which reduces the zero resistivity (or irreversibility) field.

(Some figures in this article are in colour only in the electronic version)

1. Introduction

Magnesium diboride is an interesting material for applications. It is cheap and can potentially be operated at higher temperatures than the conventional superconductors NbTi or Nb$_3$Sn. Unfortunately, the upper critical field, B_{c2}, of pure MgB$_2$ is comparatively small ($\sim$14 T at 0 K [1]) and the upper critical field anisotropy [1] leads to a strong magnetic field dependence of the critical current density, J_c [2]. Thus the in-field performance of clean MgB$_2$ is modest, but can be improved by the introduction of small impurities, which act as scattering centers, reduce the mean free path of the charge carriers and, therefore, enhance B_{c2}. Today's best wires already touch the performance of NbTi [3, 4]. It was shown in [1] that the critical currents in MgB$_2$ are still smaller by a factor of about five compared to expectations for an optimized material. It is non-trivial to decide whether this difference is caused by comparatively weak pinning (compared to optimum) or by a reduced cross section over which the currents flow [5], but it seems that the latter is more important [1]. In fact, the density of the superconducting filaments in typical wires or tapes is often only around half the theoretical one and secondary phases, especially oxides [6–8] or boron-rich compounds [8], are found at grain boundaries. These impurity phases are expected to block the current flow. The corresponding reduction in cross section is usually called the reduced area or connectivity problem and can be quantified by a factor $A_{con} \leqslant 1$. The current has to meander between the well-connected grains and this current percolation is amplified by the upper critical field anisotropy of MgB$_2$, when a magnetic field is applied. The grains of the current carrying 'backbone' attain different properties according to their crystallographic orientation with respect to the applied field. A model for the current flow in MgB$_2$ was proposed in [2]. It is based on the introduction of an effective cross section $A_p \sigma_0$ (similar to A_{con}) as a function of the fraction of superconducting grains, p, which changes with field, temperature and applied current. σ_0 denotes the geometrical cross section, thus A_p varies between 0 and 1. The original model assumed in principle that all grains (or sites in the terminology of percolation theory) consist of MgB$_2$ and are perfectly connected. If these assumptions become invalid, adoptions have to be made, which depend on the actual defect structure, as discussed in the following paragraphs.

Each non-superconducting inclusion (or pore) reduces A_{con}, which becomes an additional parameter of the model [1]. The percolation threshold p_c (defined as the minimum fraction of superconducting grains which is necessary for a continuous current path) is expected to change only if the average number of connections between neighboring (superconducting) grains is reduced. The number of connections between nearest neighbors is constant in a regular lattice and called the coordination number, K. The percolation threshold is closely related to the coordination number [9, 10]: the larger K is, the smaller is p_c.

An instructive and simple situation occurs if the morphology of the defects is comparable to the morphology of the MgB_2 grains. The structure of the system does not change, but the number of superconducting grains is reduced to $p_{MgB_2} p$. p_{MgB_2} is the fraction of MgB_2 grains and p denotes further on the superconducting fraction among the MgB_2 grains (which depends on temperature, field and current). If A_p is a simple power law of the form

$$A_p(p, p_c) = \left(\frac{p - p_c}{1 - p_c} \right)^t, \qquad (1)$$

it can be rewritten as [11]

$$
\begin{aligned}
A_p(p_{MgB_2} p, p_c) &= \left(\frac{p_{MgB_2} p - p_c}{1 - p_c} \right)^t \\
&= \left(\frac{p_{MgB_2}(p - p_c/p_{MgB_2})}{1 - p_c} \right)^t \\
&= \left(\frac{p_{MgB_2}(p - p_c^*)}{1 - p_c^*} \frac{1 - p_c^*}{1 - p_c} \right)^t \\
&= \left(\frac{p - p_c^*}{1 - p_c^*} \frac{p_{MgB_2}(1 - p_c^*)}{1 - p_c} \right)^t \\
&= \left(\frac{p - p_c^*}{1 - p_c^*} \right)^t \left(\frac{p_{MgB_2} - p_c}{1 - p_c} \right)^t \\
&= A_p(p, p_c^*) A_p(p_{MgB_2}, p_c) \\
&= A_p(p, p_c^*) A_{con}. \qquad (2)
\end{aligned}
$$

Thus, $A_p(p_{MgB_2}, p_c)$ splits into a field-and temperature-independent factor, which is just the connectivity, A_{con}, and a modified A_p needed for the percolation model [2]. A_{con} is given by the same power law as the original $A_p(p, p_c)$, with p equal to p_{MgB_2}. The percolation threshold in the modified A_p increases to $p_c^* = p_c/p_{MgB_2}$. This increase reduces the zero resistivity field and increases the field dependence of the critical currents [12]. Note that the increase of the percolation threshold is independent of the actual function of A_p, since it just results from the condition that the total fraction of superconducting grains, which is reduced by p_{MgB_2}, still has to be p_c.

The same scenario occurs if individual MgB_2 grains are completely covered by an insulating layer and disconnected from the connected matrix, p_{MgB_2} then refers to the fraction of connected MgB_2 grains.

If the insulating inclusions (the same holds for pores) and their separation are much larger than the superconducting grains, mainly A_{con} is reduced, since the average coordination number does not change significantly. Only grains neighboring these non-superconducting sites have less connections to MgB_2 grains, but their number is small, since the distance between the inclusions is assumed to be much larger than the diameter of the MgB_2 grains. The reduction in A_{con} is expected to have a similar dependence on the non-superconducting volume fraction for both small and large inclusions.

If the inclusions are much smaller than the MgB_2 grains, or if they have a totally different morphology, it is harder to predict their influence. The blockage of individual connections (not whole grains) by insulating phases is expected to result

in an increase of the percolation threshold (reduction of the average coordination number) and a reduction in A_{con}. Since the insulating layers might be much thinner than the diameter of the MgB_2 grains, a small volume fraction of secondary phases might result in a strong effect. The problem changes from site to bond percolation [13] and the volume fraction is not the ideal parameter in this case. In principle one expects a similar dependence of A_{con} on the fraction of conducting bonds, although with a different percolation threshold. (It becomes a mixed bond/site percolation problem, when a magnetic field is applied.) However, the fraction of conducting bonds is difficult to assess in real systems, but p_c of the site percolation problem might increase, because of a reduction in the average coordination number of the MgB_2 matrix.

Small inclusions (compared to the MgB_2 grain size) are not expected to influence p_c, if they do not block whole grain boundaries, but only reduce the conducting area between the grains, or if they are incorporated into the MgB_2 grains. The reduction in A_{con} might be (over-) compensated by the potential pinning capability of small defects. If these small inclusions block whole connections, because they cluster at individual grain boundaries, their influence should be similar to insulating layers.

Although the reduction of J_c by poor connectivity is quite obvious [5, 14], only a few studies were aiming at a quantitative relationship between the amount of secondary phases or pores and the corresponding reduction of the critical currents so far [15–17]. In this work, the non-superconducting volume fraction is changed by MgO particles, which were added to the MgB_2 powders before sintering. The influence of the decreasing MgB_2 volume fraction on the resistivity and on the superconducting properties is investigated and described by changes in p_c and A_p.

2. Experimental details

Powders of MgB_2 (Alfa Aesar, 98%, −325 Mesh) and MgO (Alfa Aesar, 99.95%, −325 Mesh) were weighed, mixed and pressed uniaxially with 750 MPa. The nominal MgO content ranged from 0 to 60 vol%. The pressed pellets had a diameter of 13 mm and a thickness of around 2.6 mm. Each sample was placed into an iron container and sintered separately in argon atmosphere for 10 h at 1035 °C. The temperature was ramped up at 500 °C h^{-1}. The sample cooled down slowly after the heat treatment (within a few hours). The iron container was necessary to prevent magnesium loss, which was monitored by comparing the weight of the pellet prior to and after sintering. A stripe (typically $10 \times 1.6 \times 1.5$ mm^3) was cut from the central part of the sample for the resistive measurements. A slice (around $2 \times 1.5 \times 0.4$ mm^3) was prepared from the central part of the stripe after the resistive measurements for the assessment of the critical current density.

The nominal volume fraction of MgB_2 was calculated from the weight and the theoretical density of the mixed powders. Since the density of the samples was only around 70% of the theoretical density, this nominal volume fraction strongly overestimates the real volume fraction. Therefore, this quantity is denoted as nominal content in the following.

A better estimate of the real volume fraction was calculated from the weight of the admixed MgB_2 powder, the theoretical density of MgB_2 and the final volume of the sintered pellet. (It is always close to the nominal MgB_2 content times 0.7.) The real volume fraction of MgB_2 might be smaller, if MgB_2 partly decomposes or reacts with MgO during sintering. However, the volume fraction used in the following always refers to this calculation.

The temperature dependence of the ac susceptibility was measured in a commercial SQUID magnetometer (Quantum Design), with an amplitude of 30 μT. The demagnetization factor of each sample geometry (typical dimensions: $2 \times 2 \times 1.5$ mm^3) was calculated numerically (between 0.45 and 0.65) in order to determine the susceptibility correctly.

The resistivity was monitored at various fixed applied fields between 0 and 15 T, while ramping the temperature down at 10 K h^{-1}. Current and voltage contacts were made with silver paste. An electric field of around 15 μV cm^{-1} (max. 25, min. 5 μV cm^{-1}) was applied at room temperature to ensure that the (local) current density within the current path remains comparable for all MgO content. This procedure is based on the assumption that the intrinsic resistivity of the conducting material (MgB_2), ρ, does not change and that the increase in resistance results only from the reduction in cross section of the actual current path. The (local) current density J is then only given by the electric field E ($\vec{E} = \rho \vec{J}$). The current (100 nA– 10 mA) was then kept constant during the measurement. The corresponding (local) current density can be estimated to be around 7×10^3 A m^{-2}. A linear fit to $\rho(T)$ was made in the range $0.5\rho_n < \rho < 0.9\rho_n$. Extrapolation to the normal state resistivity $\rho_n(T)$ defined the (onset) transition temperature T_c. $\rho_n(T)$ was also obtained by linear extrapolation of the normal state resistivity above the transition to lower temperatures. The temperature, where the resistivity apparently reduces to zero, $T_{\rho=0}$ (zero resistivity temperature), was evaluated. The upper critical field and the zero resistivity field were obtained by inversion of $T_c(B)$ and $T_{\rho=0}(B)$, respectively.

Magnetization loops were recorded in a commercial vibrating sample magnetometer (VSM) at 5 and 20 K. The field was ramped at 0.25 T min^{-1} from −2 to 5 T and back to zero. The critical current density was calculated from the irreversible component of the magnetic moment using the Bean model [18]. A self-field correction was made numerically [19].

A small anisotropy of the properties was detected in the magnetization measurements. The zero resistivity field is lower by about 3% in the pure MgB_2 sample when the field is oriented parallel to the direction of the uniaxial pressure, than after rotation by 90°. This means that the induced texture is very weak and can be neglected in the following. The self-field critical current density is higher by about 75% in the parallel orientation. This significant difference is possibly caused by small cracks. Large cracks were visible in some pellets, which were perpendicular to the direction of the pressure (at least in the center of the pellet, from where the samples were cut). This is illustrated in figure 1(a). No samples with large visible cracks were used in the measurements, but it is not unlikely that small cracks were present in all samples, which reduce currents flowing perpendicular to the crack direction
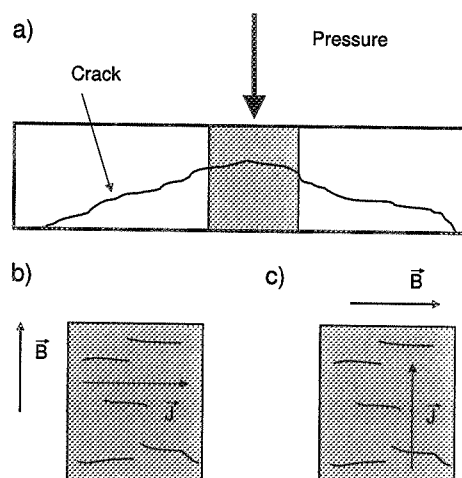

Figure 1. Large crack in the pellet after pressing (a). Samples for measurements were cut from the center of the pellet (gray area). Orientation of the small cracks, magnetic field and currents during resistive (b) and magnetization (c) measurements.

(figure 1(c)). Only in magnetic fields parallel to the former direction of the pressure do the induced shielding currents always flow parallel to the cracks, which does not result in a suppression of J_c (figure 1(b)).

The magnetization measurements of all other samples were performed only for one orientation, i.e. with the smallest dimension parallel to the applied field. The field was always perpendicular to the direction of the pressure (figure 1(c)). In order to check for possible influences of the geometry of the specimen on the derived current densities, the pure MgB_2 sample was also measured with the smallest dimension (and the direction of pressure, which was the longest dimension) perpendicular to the applied field. Nearly identical results were obtained in this case.

The current was applied perpendicular and the field parallel to the direction of pressure during the resistivity measurements (figure 1(b)).

3. Results and discussion

The ac susceptibility of samples with different MgB_2 content is plotted in figure 2. The labels refer to the nominal MgB_2 content. The samples containing 0 and 10 vol% MgO nearly (−0.925) reach the ideal value, −1, for complete flux expulsion at low temperatures. The slightly smaller value could result from an overestimation of each dimension by only 2.5%, or by the imperfect geometry of the sample (the numerical calculation of the demagnetization factor is based on a perfect cuboid). The low temperature susceptibility then decreases continuously with MgB_2 content, down to 55% MgB_2. This is the first sample with a quite significant broadening of the transition and a non-constant susceptibility below 25 K. The further decrease in MgB_2 content led to an abrupt reduction of the susceptibility. The samples with 55 and 47.5% MgB_2 behave quite similarly above 37 K, but the susceptibility differs by a factor of about 2.7 at low
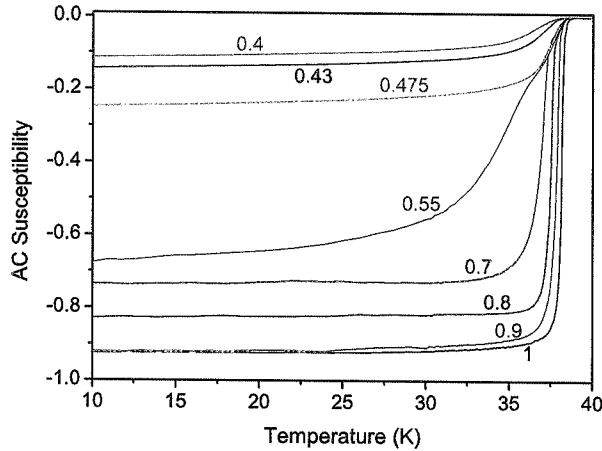
Figure 2. Change of the ac susceptibility with the nominal MgB$_2$ content, which is given by the labels.
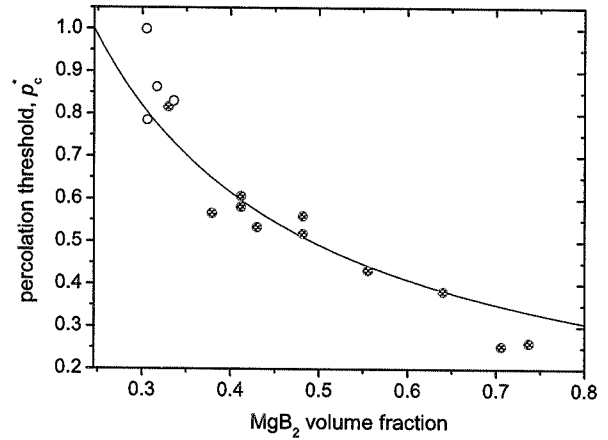

Figure 3. The percolation threshold as a function of the volume fraction of MgB$_2$, p_{MgB_2}. The open symbols represent data from samples with finite resistivity in the superconducting state.

temperatures. Thus, macroscopic shielding was established in the 55% sample at low temperatures, while for lower MgB$_2$ content the length scale of shielding obviously changes. Note that all corresponding transport samples were macroscopically superconducting (zero resistivity); only the 40% MgB$_2$ sample was apparently insulating.

The superconducting transition temperature, T_c, continuously decreases with MgB$_2$ content, although the maximum shift is only about 0.5 K near the onset of the transition (first points deviating from zero). A larger reduction of T_c was observed at the onset of the resistive transition: from 38.7 to 37.8 K, for 100% and 46% MgB$_2$, respectively. Zero resistivity was observed at 38 and 34.6 K. The residual resistivity ratio decreased from 3.7 in the pure to 1.9 in the 46% sample and the normalized resistivity $\rho_{norm} := \rho(40\,\text{K})/\Delta\rho$ increased by a factor of 3. The phonon contribution to the resistivity, $\Delta\rho := \rho(300\,\text{K}) - \rho(40\,\text{K})$, is expected to hardly change with disorder [1]: thus the increase in ρ_{norm} reflects the enhancement of the residual resistivity, ρ_0 ($\sim\rho(40\,\text{K})$ in the present samples). A linear dependence of T_c on ρ_{norm} is observed, similar to previous reports [1, 20–22]. The corresponding increase in upper critical field is observed in the present samples, too. The changes indicate that the intrinsic properties of the MgB$_2$ grains changed somewhat, either by a slight loss of magnesium, or by any reaction between the two different powders. In any case impurity scattering is increased, which complicates the situation, since not only the volume fraction of MgB$_2$ is varied. In particular the upper critical field anisotropy, γ, is needed in the following. It is known to be sensitive to impurity scattering [23], but it can be estimated from T_c by [1]

$$\gamma(T_c) = \frac{t_c^2 + 16.7t_c(1 - t_c)}{3.88 - 3.724t_c},\qquad(3)$$

with $t_c := T_c/T_{c0}$ and $T_{c0} = 39.43$ K.

The percolation cross section p_c^* can be estimated from the ratio between the upper critical field and the zero resistivity

field, if γ is known [12]:

$$p_c^* = \sqrt{\frac{\frac{B_{c2}^2}{B_{\rho=0}^2} - 1}{\gamma^2 - 1}}.\qquad(4)$$

For highly diluted MgB$_2$, when p_c^* is close to 1, γ approaches $B_{c2}/B_{\rho=0}$. The highest value for this ratio was 4.75, as found in the sample with the highest, but still finite, resistivity (44% MgB$_2$). Exactly the same value for the anisotropy is obtained from equation (3) with the midpoint T_c (defined as the temperature where the resistivity drops to $0.5\rho_0$). The midpoint T_c is a reasonable criterion, since it accounts for material inhomogeneities. In this particular sample it was lower by 0.8 K than the onset T_c. This excellent agreement justifies the application of equation (3) to estimate γ of all samples from the midpoint T_c. The percolation threshold p_c^* was then calculated from the ratio of the upper critical field and the zero resistivity field (equation (4)) at 15 K. This temperature was chosen to avoid extrapolation of $B_{c2}(T)$ to lower temperatures and γ was shown not to change significantly at lower temperatures.

Figure 3 presents p_c^* as a function of the MgB$_2$ volume fraction. The line graph represents the theoretical behavior $p_c^* = p_c/p_{MgB_2}$ with $p_c = 0.246$ as obtained by a fit to the solid circles. This value corresponds formally to the percolation threshold of dense pure MgB$_2$ ($p_{MgB_2} = 1$). The open circles were neglected, since they represent data from samples with a constant but finite resistivity below the superconducting transition in zero field. This indicates either the presence of conducting but not superconducting phases in the remaining highly percolative current path, or normal conducting tunnel currents (see below). With these data points, p_c changes to 0.259. In the following we assume $p_c = 0.25$, which is in between the percolation threshold of a simple cubic lattice ($K = 6$, $p_c = 0.311$) and a face-centered cubic or hexagonal close-packed lattice ($K = 12$, $p_c = 0.199$ in both cases) [9]. It is close to the theoretical p_c of a body-centered cubic lattice ($K = 8$, $p_c = 0.246$). An average coordination number of 8 seems reasonable in a typical irregular structure.
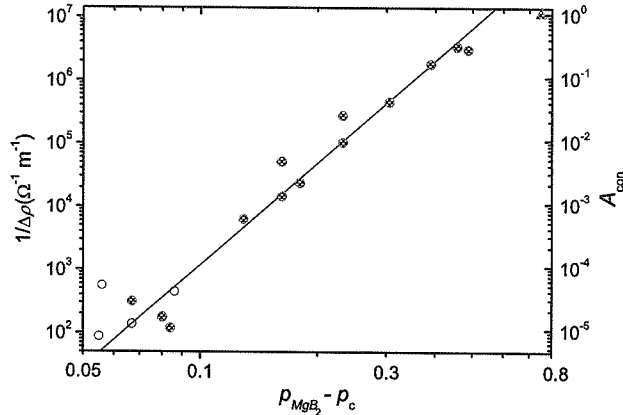
Figure 4. Change of the conductivity with the MgB$_2$ volume fraction. The line is a fit to the universal behavior (equation (1)) with $t = 5.4$. The open symbols correspond to samples with finite resistivity in the superconducting state. The triangle in the upper right corner is the expected value for perfect connectivity (9 $\mu\Omega$ cm).

Figure 5. Influence of the nominal MgB$_2$ content (labels) on the critical current densities at 20 K.

It should be emphasized that two samples with an MgB$_2$ fraction below 0.3 (but above 0.25) were apparently insulating. This could be due to finite size effects, which are expected to result in a larger percolation threshold, or simply by the difficulty in making contacts on the fragile spanning cluster, which could be even disrupted during cooling after sintering due to mechanical tensions induced by different thermal expansion coefficients of MgO and MgB$_2$.

The two points corresponding to pure MgB$_2$ ($p_{MgB_2} > 0.7$) were not taken into account for the fitting in either case, because they obviously deviate from the behavior of the mixed samples (figure 3). The added MgO powder seems to reduce the average coordination number, possibly due to a different morphology of grains, or by a reaction with MgB$_2$, resulting in a new phase which blocks grain boundaries for supercurrents. The non-zero resistivity of some samples is another hint for the latter scenario. However, extrapolating p_c^* of the pure MgB$_2$ samples to the perfectly dense case (again with $p_c^* = p_c/p_{MgB_2}$, thus the values of these two points are multiplied by about 0.7), one finds a percolation threshold of about 0.19, which is low but not unrealistic, since p_c was found to be even lower in some systems [17, 24].

The phonon contribution to the resistivity was introduced as a measure of the effective area in MgB$_2$ [5], since $1/\Delta\rho$ should be proportional to the cross section over which the current flows, at least if no other conducting phases exist in the sample. $\Delta\rho$ is not expected to be influenced by the observed changes of the superconducting properties.

Figure 4 illustrates that the conductivity can be nicely described by the universal behavior (equation (1)). The best approximating (only zero resistivity samples) transport exponent, t, is 5.4, which is much higher than the theoretically universal value of $\sim$2 in regular three-dimensional systems [13]. The transport exponent in disordered continuum systems, which can be described by the so-called Swiss-cheese model, is predicted to be only slightly higher, around 2.5 [25]. However, larger values were frequently observed experimentally in real
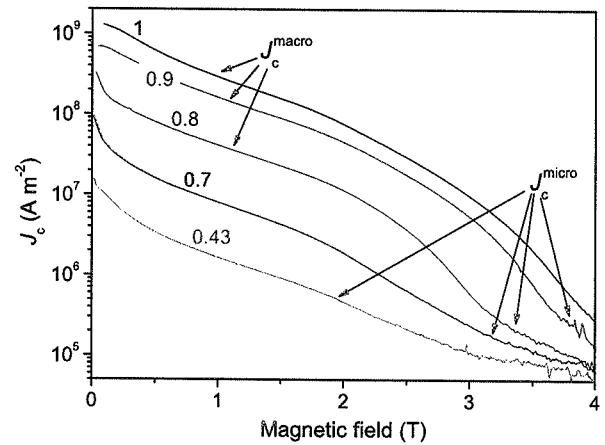
systems [17, 24, 26]. The universal behavior is predicted only for the vicinity of p_c (which is not accessible to the present experiment). Thus the application to rather high fractions, p, is problematic and might result in higher transport exponents. As shown recently [27], the transport exponent retains its universal value only very close to p_c, if tunnel currents are taken into account and much higher apparent values are expected at higher fractions p. One might speculate that connections, which are blocked by small MgO particles or layers, might be transparent for tunneling currents, leading to this high transport exponent. This could also explain the finite resistivity of some samples well below T_c, if the local current exceeds the maximum Josephson current.

Yamamoto *et al* [15] found a larger percolation threshold of 0.31, but a much weaker dependence of $\Delta\rho$ (and J_c) on the volume fraction of MgB$_2$, which was varied between 0.44 and 0.87 by different preparation techniques (all samples were prepared *in situ*). Their non-superconducting volume consisted mainly of pores. Thus, it is obvious that pores and MgO particles have a different influence on the properties of MgB$_2$. This is also supported by the present data, since extrapolation of the data to $p_{MgB_2} = 1$ does not lead to the expected value of $\Delta\rho \sim 9$ $\mu\Omega$ cm (triangle in figure 4), but to 1.67 $\mu\Omega$ cm, although this discrepancy could result also from a change in behavior near $p_{MgB_2} = 1$. However, we also found a smaller extrapolated p_c in the pure MgB$_2$ samples (see above).

The critical current densities at 20 K are presented in figure 5. J_c at self-field is around 10^9 A m^{-2} in the pure sample, thus considerably smaller than in typical *in situ* prepared samples. J_c in a sample of comparable connectivity ($\Delta\rho$ was 29 $\mu\Omega$ cm in our pure sample) was found to be around four times higher in [15]. This can be explained by the different grain size. The grain size of *in situ* prepared samples is generally smaller (e.g. $\sim$100 nm [15]) than in *ex situ* samples (e.g. up to 1 μm [6]). In particular our long heat treatment favors grain growth. Thus, the density of grain boundaries, which are the dominant pinning centers in MgB$_2$, is expected to be low in the present samples.

The critical current densities decrease with decreasing MgB$_2$ content. The steep slope at higher fields (e.g. between

2 and 3 T in sample 0.8) gradually disappears. This strong decrease in J_c can be associated with the fast reduction in effective cross section (for high currents). At higher fields, after the decomposition of the spanning cluster, $J_c(B)$ becomes flatter again, but the currents are now flowing on a different length scale, namely on disconnected clusters of grains. Note that the evaluation of J_c assumes the currents to flow macroscopically around the sample. One obtains the corresponding macroscopic current density J_c^{macro}, if this condition is fulfilled. The evaluation becomes invalid if the currents, which flow on a smaller length scale, J_c^{micro}, generate a significant contribution to the total magnetic moment [28]. These additional currents lead to an overestimation of the macroscopic critical current density, because they increase the measured moment. On the other hand, J_c^{micro} is underestimated, if the macroscopic currents become small or even zero, because the area enclosed by the microcurrents is much smaller than the sample geometry and *a priori* unknown. Only if the macroscopic currents dominate is the correct J_c^{macro} obtained; in all other cases the derived *magnetic* J_c is wrong. Nevertheless, this *magnetic* J_c illustrates the differences between samples with and without large macroscopic currents. Sample 0.43 was apparently insulating, thus the spanning cluster is very weak or not existing at all, even at zero field. Currents flowing on a microscopic length scale are expected under all conditions (when superconducting grains exist), but it depends on the field and the amount of MgB_2 whether they give a negligible (small fields and large MgB_2 concentration), important, dominant or even the only contribution (small MgB_2 concentration or large fields) to the signal. Their importance generally increases with increasing field and decreasing MgB_2 concentration. The slope of $J_c(B)$ is similar in all samples up to about 2 T (except in the low field region, where geometry-dependent self-field effects become important), since the length scale of current flow does not change (figure 5). The decomposition of the spanning cluster, if existing, always starts near B_{c2}/γ. In principle the weakening of the spanning cluster starts exactly at B_{c2}/γ, where the number of superconducting grains p starts to decrease, but if p is assumed to depend on J [2] (p decreases with J) the 'spanning cluster for high currents' decomposes at smaller fields. After the destruction of the spanning cluster, the average size and number of the disconnected clusters further depend on $p_{MgB_2}p(B, J)$, leading to different slopes of the *magnetic* J_c at high fields. Note that $B_{\rho=0}$ derived from resistive measurements falls into this region, e.g. 4.5 T in sample 0.8. The influence of the macroscopic currents in the remaining spanning cluster on the magnetization is small: they might even be described by a network of tunneling junctions [5].

The derived critical currents are a useful approximation for the macroscopic currents at low MgO concentrations and low magnetic fields. $J_c(0.5 \text{ T}, 5 \text{ K})$ is plotted as a function of the MgB_2 volume fraction (reduced by $p_c = 0.25$) in figure 6. The transport exponent $t = 5.4$ is illustrated by the line graph and describes the data very well, down to a volume fraction of about 0.5. The influence of the microscopically circulating currents becomes dominant at lower concentrations.
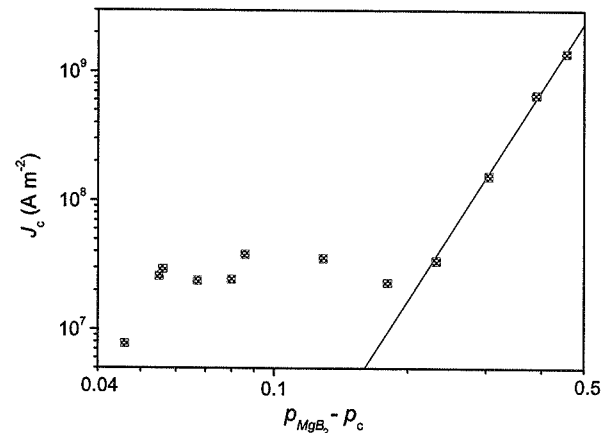

Figure 6. Critical current densities at 5 K and 0.5 T. p_c was assumed to be 0.25.

The observation of the same reduction in cross section for normal and supercurrents, which was also found for porous samples [15], supports the idea of using $\Delta\rho$ to estimate the reduction in J_c due to a reduced connectivity.

4. Conclusions

The percolative current transport was investigated in mixed MgB_2/MgO samples. The superconducting transition width increases, susceptibility, critical current, and conductivity decrease with increasing MgO content. The expected change in the relevant length scale for shielding currents was observed in magnetization measurements. An unusually high transport exponent of 5.4 and a percolation threshold of about 0.25 were found. The latter is higher than in porous MgB_2 ($p_c < 0.2$), which has a smaller dependence of the transport properties on the superconducting volume fraction than the mixed MgB_2/MgO samples. A reduction in J_c by a factor of 2 can be expected by the presence of only 10% MgO.

The phonon contribution to the resistivity was confirmed to be a useful measure for the decrease in J_c due to poor connectivity or density.

References

[1] Eisterer M 2007 *Supercond. Sci. Technol.* **20** R47
[2] Eisterer M, Zehetmayer M and Weber H W 2003 *Phys. Rev. Lett.* **90** 247002
[3] Herrmann M, Haessler W, Rodig C, Gruner W, Holzapfel B and Ludwig S 2007 *Appl. Phys. Lett.* **91** 082507
[4] Hur J M, Togano K, Matsumoto A, Kumakura H, Wada H and Kimura K 2008 *Supercond. Sci. Technol.* **21** 032001
[5] Rowell J M 2003 *Supercond. Sci. Technol.* **16** R17

[6] Birajdar B, Peranio N and Eibl O 2008 *Supercond. Sci. Technol.* 21 073001

[7] Jiang J, Senkowicz B J, Larbalestier D C and Hellstrom E E 2006 *Supercond. Sci. Technol.* 19 L33

[8] Klie R F, Idrobo J C, Browning N D, Regan K A, Rogado N S and Cava R J 2001 *Appl. Phys. Lett.* 79 1837

[9] van der Marck S C 1997 *Phys. Rev.* E 55 1514

[10] Wierman J C and Naor D P 2005 *Phys. Rev.* E 71 036143

[11] Eisterer M, Schöppl K R, Weber H W, Sumption M D and Bhatia M 2007 *IEEE Trans. Appl. Supercond.* 17 2814

[12] Eisterer M, Krutzler C and Weber H W 2005 *J. Appl. Phys.* 98 033906

[13] Stauffer D and Aharony A 1992 *Introduction to Percolation Theory* (London: Taylor and Francis)

[14] Rowell J M, Xu S Y, Zeng X H, Pogrebnyakov A V, Li Qi, Xi X X, Redwig J M, Tian W and Pan X 2003 *Appl. Phys. Lett.* 83 102

[15] Yamamoto A, Shimoyama J, Kishio K and Matsushita T 2007 *Supercond. Sci. Technol.* 20 658

[16] Matsushita T, Kiuchi M, Yamamoto A, Shimoyama J-I and Kishio K 2008 *Supercond. Sci. Technol.* 21 015008

[17] Grinenko V, Krasnoperov E P, Stoliarov V A, Bush A A and Mikhajlov B P 2006 *Solid State Commun.* 138 461

[18] Bean C P 1964 *Rev. Mod. Phys.* 36 31

[19] Wiesinger H P, Sauerzopf F M and Weber H W 1992 *Physica* C 203 121

[20] Eisterer M, Müller R, Schöppl R, Weber H W, Soltanian S and Dou S X 2007 *Supercond. Sci. Technol.* 20 117

[21] Gandikota R *et al* 2005 *Appl. Phys. Lett.* 86 012508

[22] Tarantini C *et al* 2006 *Phys. Rev.* B 73 134518

[23] Krutzler C, Zehetmayer M, Eisterer M, Weber H W, Zhigadlo N D and Karpinski J 2007 *Phys. Rev.* B 75 224510

[24] Lee S-I, Song Yi, Noh T W, Chen X-D and Gaines J R 1986 *Phys. Rev.* B 34 6719

[25] Halperin B I, Feng S and Sen P N 1985 *Phys. Rev. Lett.* 54 2391

[26] Vionnet-Menot S, Grimaldi C, Maeder T, Strässler S and Ryser P 2005 *Phys. Rev.* B 71 064201

[27] Johner N, Grimaldi C, Balberg I and Ryser P 2008 *Phys. Rev.* B 77 174204

[28] Horvat J, Yeoh W K, Kim J H and Dou S X 2008 *Supercond. Sci. Technol.* 21 065003